JOURNAL OF CATALYSIS 113, 72–81 (1988)

Photocatalytic Deposition of Silver on Powder Titania: Consequences for the Recovery of Silver

JEAN-MARIE HERRMANN, JEAN DISDIER, AND PIERRE PICHAT

Equipe CNRS Photocatalyse, Ecole Centrale de Lyon, BP 163, 69131 Ecully Cedex, France

Received December 8, 1987; revised March 21, 1988

The effects of various parameters on the photoassisted reduction of silver ions to metallic deposits on powder titanium dioxide has been studied. The initial deposition rate (i) varied with the starting concentration of Ag^+ ions according to a Langmuir–Hinshelwood mechanism, (ii) was almost independent of the temperature around 300 K, and (iii) was proportional to the radiant flux (300 nm $< \lambda <$ 400 nm) of photons absorbable by TiO_2, at least up to a value of 7.6×10^{15} photons s^{-1} cm^{-2}. For the same illumination conditions, an apparent initial quantum yield of 0.16 was calculated at room temperature in the case of complete coverage of the surface by Ag^+ ions. Transmission electron microscopy revealed that silver initially formed particles between 3 and 8 nm in diameter. For larger amounts of silver deposited and longer illumination times, large crystallites (up to 400 nm) were also observed. This prevented the photosensitive surface from being substantially covered and, for instance, a silver-to-titania mass ratio of ca. 2.4 was reached without a decrease in the deposition rate. This phenomenon, as well as the removal of silver ions down to the detection limit, supports the possible use of this method for the recovery of silver from dilute aqueous solutions. In this connection, preliminary experiments showed that silver was selectively extracted from equimolar solutions of Ag^+ and Cu^{2+} ions (cf. electrolytic baths) and that it was also recovered in the presence of thiosulfate ions (cf. photographic fixing baths).

INTRODUCTION

Because of appropriate redox potentials, a certain number of metal cations can be reduced by the free electrons created by band gap illumination of common semiconductors. This phenomenon has been known for more than 20 years (*1–4*) and it has often been employed to obtain metals deposited on semiconductor powders or colloids *in situ*, with a view to increase the rate of steps involving hydrogen in photocatalytic reactions.

Generally, oxidizable additives (hole scavengers) were added to improve the rate of deposition. It has even been claimed that in their absence there is no reduction of platinum on a titanium dioxide sample (*5*). Currently, photodeposition is reexamined, not only for the preparation of well-dispersed metallic (*6–10*) or bimetallic (*10*) supported catalysts, but also, to a larger extent, for the recovery of noble or toxic metals. In this respect, more work on the influence of the parameters affecting the kinetics of the photodeposition and the morphology of the metal deposits has been undertaken.

If we limit the literature survey to noble metal photodeposition on powder semiconductors with the objective of recovering metal, recent studies have dealt with various salts or complexes of gold, in the absence (*11*) or presence of cyanide ions (*12*), rhodium (*13*), palladium (*13*), and platinum (*14*). Selective recovery of a given metal by this method was also shown in the case of gold extracted from a mixture of Cu, Ni, and Zn ions (*11*) and for Pt removed from Pt–Rh solution (*13*). Titania was generally used.

In the particular case of silver, several papers have been devoted to its photodeposition, mainly on ZnO (*15–17*) and on TiO_2 (*1, 15, 18–21*). The relevant information is discussed throughout this article whenever necessary.

The present work on the photodeposition

0021-9517/88 $3.00

of silver was undertaken to extend the previous detailed study concerning that of platinum from various complexes (*14*) and thereby to look for similarities and differences between these two metals. An anatase sample was chosen as a semiconductor because of its efficiency, its stability in UV-illuminated aqueous solutions, and its low cost. In addition, preliminary experiments were carried out with a view to possible implementation of the method for silver recovery from diluted aqueous solutions. The mass of silver recovered per unit mass of titanium dioxide was determined. High loadings were obtained because of the formation of large metal crystallites as shown by transmission electron microscopy. Silver was selectively recovered from Ag^+–Cu^{2+} mixtures, and the presence of thiosulfate ions, as in photograpic fixing baths, did not hinder its deposition.

EXPERIMENTAL

Materials. TiO_2 was nonporous Degussa P-25, mainly anatase, with a surface area of 50 m^2 g^{-1}. Silver solutions were prepared with $AgNO_3$ (Merck) of pure reagent grade.

Photoreactor. The photodeposition of silver was carried out in a Pyrex flask of ca. 100 cm^3 with a bottom optical window transparent to wavelengths greater than or equal to 300 nm. This reactor could be connected to a vacuum line or to a gas chromatograph for analysis of evolved gases. The slurry was vigorously agitated with a magnetic stirrer. A Philips HPK 125-W mercury lamp was employed.

Analyses. The reaction rate was followed by using atomic absorption spectrometry (AAS) to analyze the remaining Ag^+ ions in the solution obtained after centrifugation at 12,000 rpm and/or by measurement of the concentration of protons released in the solution [see Eq. (2)]. The oxygen evolved was sometimes measured by on-line gas chromatography. In certain cases, the amount of deposited silver was also determined by AAS analysis of the solution which was obtained by recovering the solid from the slurry by centrifugation, washing it three times with distilled water, and dissolving it in HF and aqua regia.

Procedure. Unless otherwise indicated, 50 mg of TiO_2 was suspended in 10 cm^3 of Ag solution. This concentration in TiO_2 provided complete absorption of the light for the photoreactor used. The gas phase was evacuated for 2 min, while the solution was stirred. The suspension was maintained in the dark under static vacuum for 15 min to allow the evolution of dissolved or reversibly adsorbed gases which were subsequently evacuated for a second period of 2 min. No oxygen was chromatographically detected after this procedure.

RESULTS AND DISCUSSION

Preliminary Remarks

The reactant did not absorb at wavelengths greater than 300 nm; hence no correction was needed to determine the efficient radiant flux. Since adsorption is the preliminary step in any photocatalytic system, Ag^+ adsorption was determined by analyzing this supernatant solution after stirring slurries containing various concentrations c of silver in the dark at natural pH (ca. 4.5) for 15 min. Maximum adsorption was found at ca. $c = 4 \times 10^{-4}$ M, corresponding to 0.44 Ag^+/nm^2, i.e., about one-tenth of the surface density of OH groups (*22, 23*). Simultaneously the pH decreased, which was indicative of the replacement of surface protons by silver ions:

$$TiOH + Ag^+ \rightleftarrows TiO\text{–}Ag + H^+ \quad (1)$$

Stoichiometry of the Photodeposition

On illumination, the suspension turned rapidly from white to brown. Figure 1 shows the variations of photodeposited silver, released protons, and evolved oxygen. For a starting concentration of 10^{-3} M, silver was removed from the solution within about 10 min and an equivalent number of protons appeared in the solution, as expected from

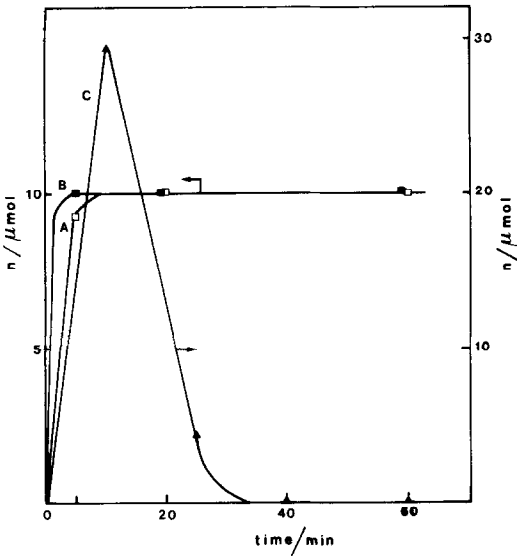

FIG. 1. Kinetics of photodeposition of Ag. Variations in the amounts of silver deposited versus time (A), H^+ released (B), and O_2 evolved (C). Conditions: 50 mg of TiO_2 in 10 cm^3 of 10^{-3} M $AgNO_3$.

$$Ag^+_{(ads)} + \tfrac{1}{2}H_2O \xrightarrow[TiO_2]{h\nu} Ag^\circ + H^+ + \tfrac{1}{4}O_2(g) \qquad (2)$$

In contrast, the amount of oxygen evolved did not follow the stoichiometry of Eq. (2). As in the case of platinum photodeposition (*14*), the initial increase in oxygen pressure (Fig. 1), which is greater than that expected from the stoichiometry, can be interpreted in terms of photodesorption of ionosorbed oxygen species remaining at the surface of titania, even after the evacuation preceding the illumination:

$$TiO_2 + h\nu \rightarrow e^- + p^+ \qquad (h\nu \geq E_G) \qquad (3)$$

$$O_x^- + p^+ \rightarrow (x/2)O_2\,(g) \qquad x = 1, 2 \qquad (4)$$

This photodesorption is beneficial for the photodeposition of silver, since it consumes holes and thus decreases the electron–hole recombination. The subsequent decrease in oxygen pressure (Fig. 1) corresponds to a period of time when most Ag^+ ions have been reduced and accordingly electrons are not predominantly captured by these ions. Oxygen, initially photodesorbed or generated by the reaction [Eq. (2)], is readsorbed on titania and also on the silver particles formed.

Effect of the Initial Concentration

The influence of the concentration on kinetics has to be determined under initial conditions since the reactor is of the static type. An illumination time of 10 min was estimated as the shortest time for a sufficiently accurate analysis. Moreover, since the quantity of reduced silver at low conversions can be of the same order of magnitude as the quantity of adsorbed silver ions, the reaction rate was determined by ph measurements [Eq. (2)]. The isotherm is presented in Fig. 2A. Similar isotherms of the Langmuir–Hinshelwood type have already been observed for Ag photodeposition on TiO_2 single crystals (*16*) and for Pt photodeposition under conditions similar to the present ones (*14*).

This implies that the photodeposition rate r obeys the equation

$$r = k\theta_{Ag} = kKC/(1 + KC) \qquad (5)$$

where θ_{Ag} is the surface coverage by Ag^+ ions, k is the rate constant (depending on the wavelength distribution and the radiant flux), and K is the adsorption constant of Ag^+ ions. These constants can be derived from the slope and the ordinate at the origin of Fig. 2B. We find that

$$k = 2.1 \times 10^{-6} \text{ mol min}^{-1}$$
$$K = 6 \times 10^2 \text{ dm}^3 \text{ mol}^{-1}.$$

This set of values is in the same range as those found for the photodeposition of platinum (*14*).

Figure 2A also indicates that the effects of other parameters on the kinetics of photodeposition should be determined at concentrations greater than or equal to 5×10^{-3} M to avoid the perturbation induced by a decreasing surface coverage by silver ions.

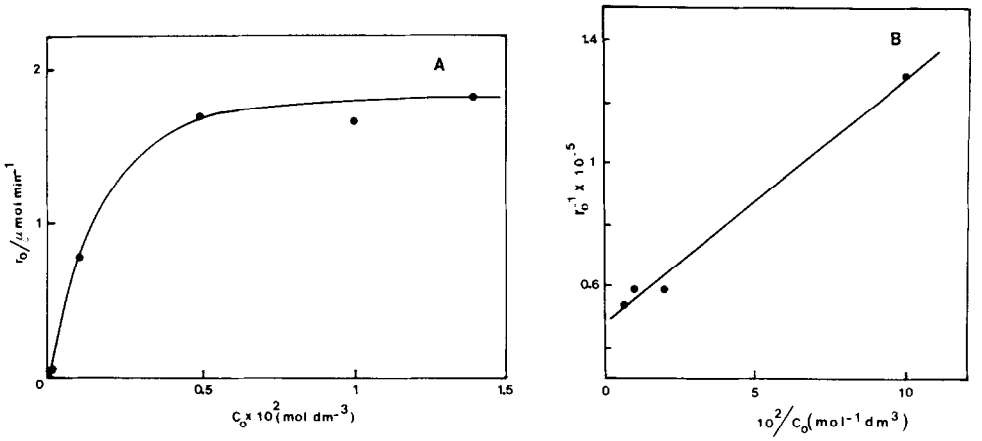

FIG. 2. (A) Initial rate of the photoassisted deposition of silver as a function of the initial concentration of $AgNO_3$. (B) Linear transform of the isotherm.

Effect of Temperature

This was studied in a jacketted photoreactor connected to a Huber HS40 thermostat. The rates were determined either by pH measurements of the suspension at room temperature or by measurement of the amount of silver deposited after 15 min illumination. The results are displayed in the Arrhenius plot in Fig. 3. The rate varies within one-tenth of an order of magnitude for $\Delta T \sim 80$ K. Between 303 and 333 K, the photodeposition rate is nearly constant, showing that the process is almost nonactivated as expected for a true photocatalytic regime (*24*). At lower temperatures ($277 \leq T \leq 303$ K), the curve indicating the release of protons into the solution can be explained by the limited beneficial effect of a rise in temperature on the desorption of protons. This is not inconsistent with the curve referring to the amounts of silver deposited on TiO_2, since these amounts include both reduced and irreversibly chemisorbed Ag^+ ions, whose adsorption is favored at lower temperatures. Similarly, for higher temperatures ($333 \leq T \leq 353$ K), the decrease in r can be ascribed to a detrimental effect of the temperature on Ag^+ adsorption. Therefore, the optimum temperature range for silver deposition under our conditions is between room temperature and ca. 333 K.

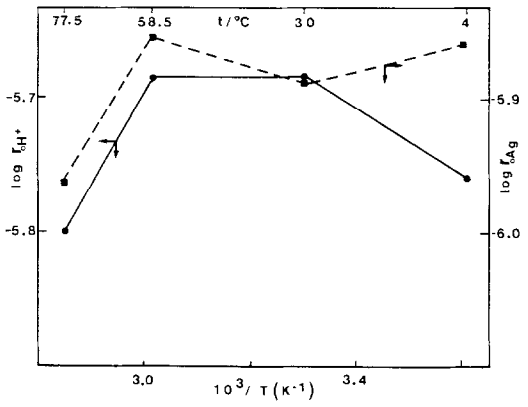

FIG. 3. Arrhenius plot of the initial rate of photodeposition of silver from 10^{-2} *M* $AgNO_3$; 50 mg of TiO_2 in 20 cm^3 of solution; illumination time = 15 min. Solid line: rate of H^+ release; dashed line: rate of silver removal from the solution.

The present Arrhenius plot differs substantially from that observed for the photodeposition of platinum (*14*) for which a straight line was obtained, corresponding to an apparent activation energy of 6 kJ mol^{-1} in the same temperature range. This difference could arise from a lower heat of adsorption of Ag^+ ions as compared with that of the chloroplatinic complex.

Effect of Radiant Flux

Quasimonochromatic light was obtained with a Corning 7-60 filter, whose maximum

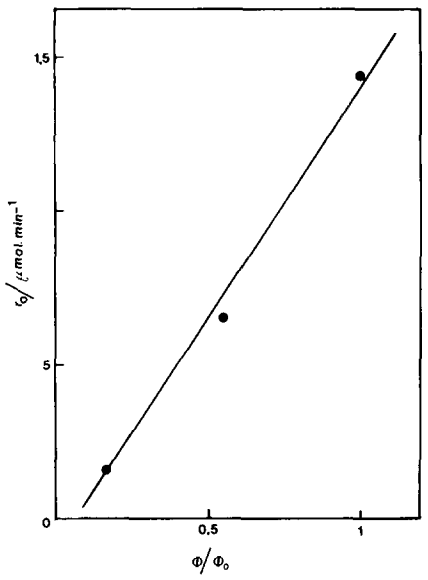

FIG. 4. Variations of the initial photodeposition rate as a function of the relative radiant flux. λ-independent attenuation of the full output of the lamp was obtained with calibrated grids. 10^{-2} *M* $AgNO_3$; illumination time = 5 min. For other conditions, see the text.

transmittance is close to that of the most intense mercury line at 365 nm. The influence of the radiant flux on the reaction rate *r*, which was derived from pH measurements, must be determined under initial conditions. Figure 4 shows that the initial reaction rate of silver photodeposition is proportional to the radiant flux Φ as previously observed, for instance, for the photodeposition of Pd on a TiO_2 single crystal (*25*) or a TiO_2 film (*26*) and for that of Pt on the same anatase powder (*14*). This implies that the second-order recombination of electrons and holes is not preponderant as corroborated by the high rate of initial photodesorption [Eq. (4)]. Otherwise, *r* would have been proportional to $\Phi^{1/2}$ (*27*).

Quantum Yield

The differential quantum yield ϕ is the ratio of the reaction rate to the incident flux of photons that can be absorbed by titania. This latter value was determined by taking into account the overall radiant flux (6.75 mW cm^{-2}), the transmission of the filter, the energy of each ray of the mercury lamp, and the absorbance of TiO_2 (in fact, use of the 7-60 Corning filter made the 365-nm line markedly preponderant). ϕ was determined (i) under initial conditions, (ii) for complete coverage by Ag^+ ions ($c_0 \geq 5 \times 10^{-3}$ *M*), (iii) at a temperature in the plateau region of Fig. 3, and (iv) with a radiant flux corresponding to the linear relationship of Fig. 4 ($\phi_0 = 7.6 \times 10^{15}$ photons s^{-1} cm^{-2}). An initial quantum yield of 0.16 was thus calculated. This value is very close to those reported for the photodeposition of silver on titania single crystal (*16, 19*) or powder (*18*). It is a lower limit since no allowance was made for light scattering by TiO_2 particles. It corresponds roughly to four times the quantum yield of platinum photodeposited under similar conditions (*14*), as expected from the ratio of the metal valences.

This quantum yield enables one to determine the energetic yield, defined as the mass of metal recovered per unit of electrical energy consumed by the lamp. Assuming no loss of the light emitted and taking into account a conversion of 20% of the electrical power into radiant power, an optimum initial energetic yield of ca. 40 g of silver per kilowatt hour or 11.1 g of silver per mega-Joule was calculated.

TiO_2 Capacity for Silver Deposition

The capacity *C* is defined as the mass of deposited metal per unit mass of support. In the first experiment, complete photodeposition of Ag on TiO_2 was achieved in order to reach a capacity of 0.42 (50 mg of TiO_2 in 20 cm^3 of 10^{-2} *M* Ag NO_3). Subsequent addition of the same quantity of Ag^+ ions doubled *C* without modification of the kinetics. In the second experiment, silver photodeposition from a more concentrated solution was carried out over 100 h without a decrease in the rate (Fig. 5). In other words, no saturation of the surface by metallic silver was reached, allowing one to reject the formation of a silver monolayer or a silver film, which would correspond to

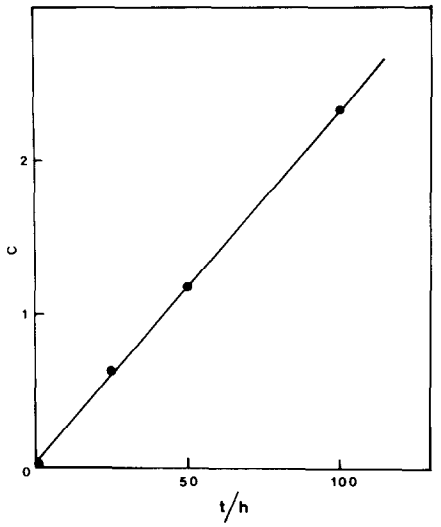

FIG. 5. Variations of the photodeposition capacity C (C = mass of deposited metal per unit of mass of support) as a function of time. Conditions: 50 mg of TiO_2 in 20 cm^3 of 10^{-1} M $AgNO_3$.

C = 0.16 or 0.52 (for a film thickness of 1 nm), respectively, and cause the progressive occultation of the titanium dioxide surface.

These long-duration experiments, together with the effects of initial concentration, temperature, and radiant flux, demonstrate that the deposition process, represented by Eq. (2), is photocatalytic according to the criteria indicated in Refs. (*28, 29*).

Transmission Electron Microscopy of the Silver Deposits

TEM examination established that silver initially deposits as small crystallites of between 3 and 8 nm in diameter on all the particles of TiO_2 (Fig. 6). In other words, well-dispersed Ag/TiO_2 catalysts, up to loadings in the range 1–2 wt%, are obtained after short periods of illumination (*10*). When the metal loading increases, huge crystallites of metal appear (up to 400 nm, i.e., much larger than the TiO_2 particles) in addition to these small particles (Fig. 7).

Large agglomerates were also found for Pt photodeposits [see Fig. 9 in Ref. (*14*)] but their shapes were different. Whereas silver particles had a regular shape, platinum gathered as "spongelike" agglomerates as if resulting from the accumulation of smaller crystallites. These differences can originate from the nature of the metals or of their ions (Ag^+ versus $(PtCl_6)^{2-}$ complexes). Since metal crystallites are enriched in photoproduced electrons (*30, 31*), they can constitute sites for the cathodic-like reduction of cations, which would progressively increase their size as observed for Pd on TiO_2 films (*31*). The fact that only one electron is needed to reduce one Ag^+ ion, instead of four for one Pt^{IV}, could favor this mechanism for silver. However, further studies are needed to elucidate the origin of the difference between Ag and Pt. These large metal particles contain the major part of the metal deposited. Consequently, the photosensitive surface is not markedly masked and high C values can be reached (Fig. 5).

Photodeposition Mechanism

The reaction steps proposed include the adsorption of Ag^+ on OH surface groups, Eq. (1); creation of electron–hole pairs, Eq. (3); and the reaction of holes with negatively charged adsorbed oxygen species, Eq. (4), and with OH^- surface species,

$$H_2O \rightleftarrows H^+ + OH^- \qquad (6)$$

$$OH^- + p^+ \rightarrow OH^\circ \rightarrow \tfrac{1}{2}H_2O + \tfrac{1}{4}O_2(g) \qquad (7)$$

whereas electrons reduce adsorbed Ag^+ ions:

$$Ag^+ + e^- \rightarrow Ag^\circ. \qquad (8)$$

Formation of small crystallites (ca. 3 nm in diameter) can occur either by agglomeration of these atoms,

$$mAg^\circ \rightarrow Ag_m \qquad (9)$$

or by cathodic-like successive reduction (*30*) as in the photographic process,

$$Ag^\circ + Ag^+ \rightarrow (Ag)_2^+ \xrightarrow{+e^-} Ag_2 + Ag^+ \rightarrow (Ag_3)^+ \xrightarrow{+e^-} Ag_3 \rightarrow \ldots \rightarrow Ag_m. \qquad (10)$$

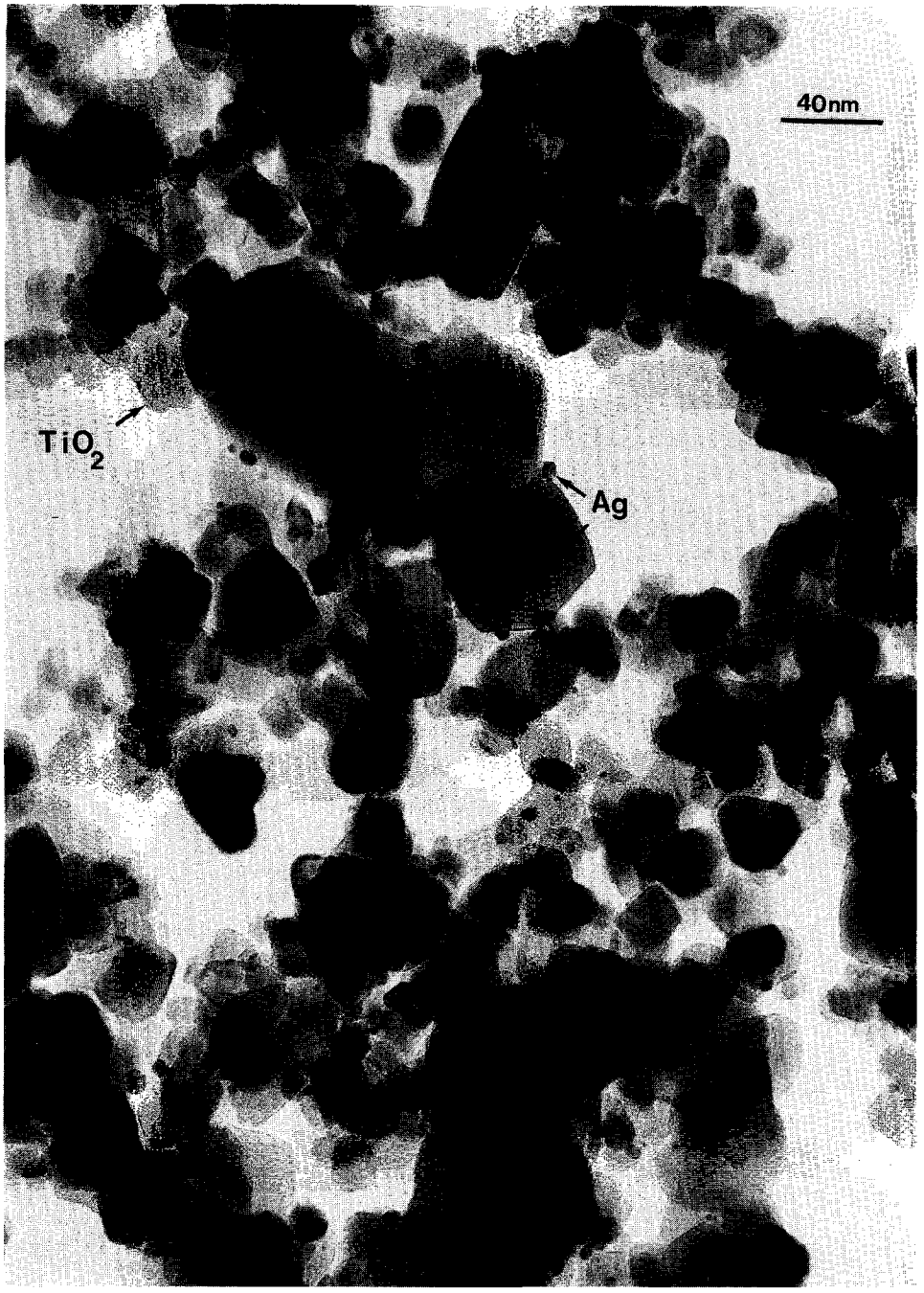

FIG. 6. Transmission electron micrograph of Ag/TiO_2 obtained after illuminating ($\lambda \geq 300$ nm) a deaerated suspension of 50 mg of TiO_2 in 10 cm^3 of 10^{-1} *M* $AgNO_3$ for 10 min. Weight percentage of Ag = ca. 2%.

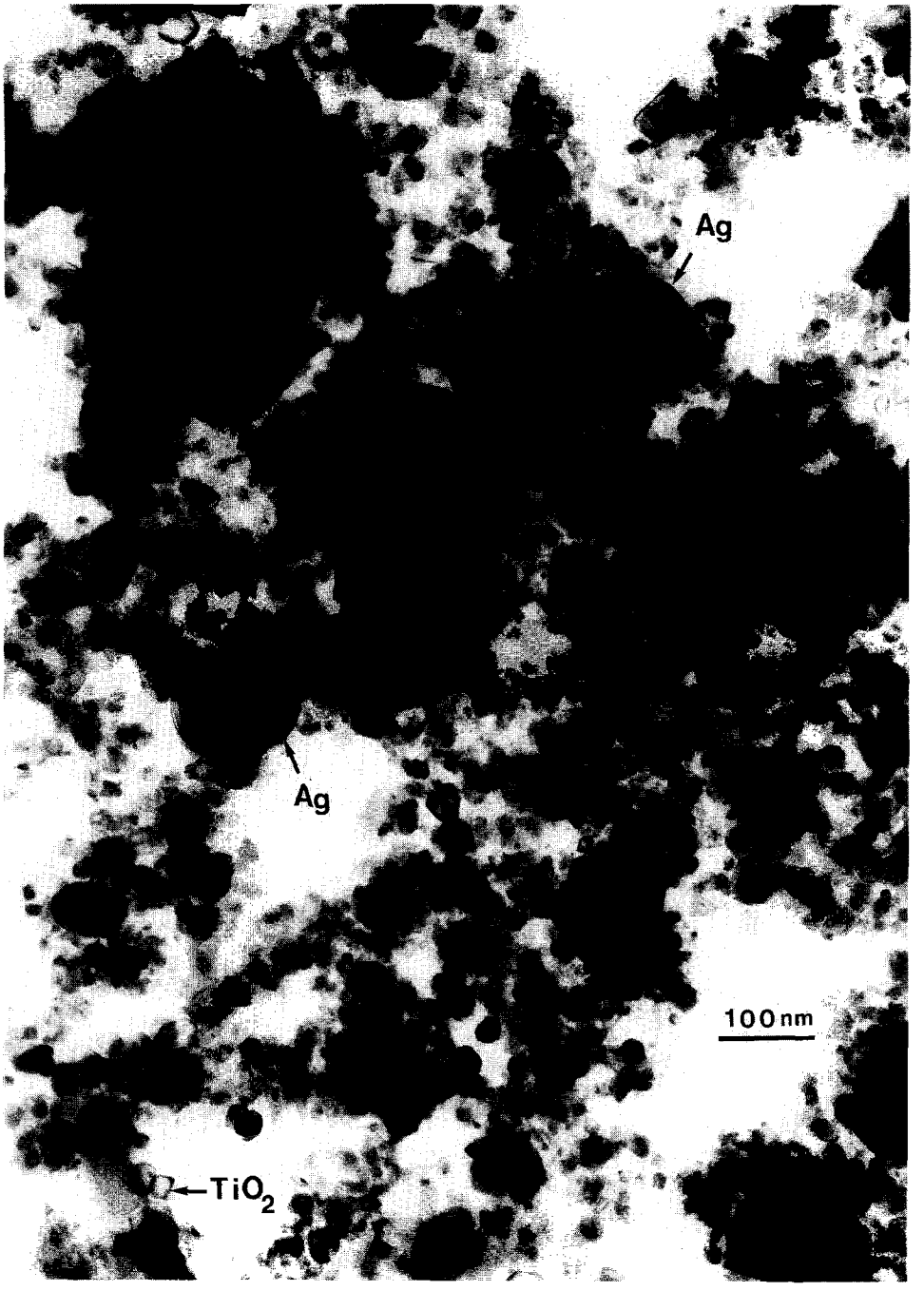

FIG. 7. As in Fig. 6 except for the $AgNO_3$ concentration (10^{-1} *M*) and the illumination time (25 h). This solid corresponds to the first point in Fig. 5. Weight percentage of Ag = ca. 38%.

TABLE 1

Separation of Silver from Copper by Photodeposition on TiO_2

$[Cu^{2+}]_0$ (*M*)	$[Ag^+]_0$ (*M*)	t_{uv} (h)	$[Cu^{2+}]_f$ (*M*)	$[Ag^+]_f$ (*M*)	Ag_f^+ (ppm)	$[Ag^+]_f/[Ag^+]_0$
10^{-3}	10^{-3}	1	10^{-3}	4.6×10^{-7}	50	4.6×10^{-4}
10^{-2}	10^{-2}	6	10^{-2}	6.5×10^{-6}	702	6.5×10^{-4}

Note. The subscripts 0 and f refer to the initial and final concentrations, respectively; t_{uv} is illumination time. Conditions: 100 mg of TiO_2 in 20 cm^3 of Cu^{2+}–Ag^+ solution.

Potential Applications

Silver recovery. In view of the capacity of titania for silver photodeposition, implementation of this method could be considered, at least in special cases. First, since in the absence of other cations and complexing anions the concentration of Ag^+ ions can be decreased to the detection limit of the atomic absorption spectrometer ($\leq$0.1 ppm), photodeposition could be used for the treatment of very diluted solutions which, for instance, have previously been subjected to classical recovery techniques.

Second, the treatment of photographic baths could also be envisaged. Indeed, total recovery of Ag was obtained from a solution containing 10^{-3} *M* Ag^+ and 2×10^{-2} *M* $S_2O_3^{2-}$ ions (conditions: 100 mg of TiO_2 in 20 cm^3; illumination time: 1 h, opened reactor). Thiosulfate ions were simultaneously oxidized to SO_4^{2-} ions.

Silver separation. Generally, industrial silver solutions contain other metal cations. In particular, copper ions are often present, especially in electrolytic baths. To assess whether silver can be recovered independently of copper, the present method was carried out using two equimolar Cu^{2+}–Ag^+ synthetic solutions of different concentrations. The results are given in Table 1. Only Ag was deposited, whereas no change in cupric ion concentration was observed. This is in agreement with previous results (*14*), which showed that copper could not photodeposit on titania, despite a slightly favorable redox potential with respect to the flat-band potential of titanium dioxide. TEM examination of the samples showed Ag crystallites of various sizes as in Figs. 6 and 7. Scanning transmission electron microscopy confirmed that metal particles were exclusively composed of silver. Some minute traces of copper could be detected, probably as Cu^{2+} adsorbed ions, in amounts too small to be deduced from chemical analysis of the final solution (Table 1).

CONCLUSION

This fundamental study combines with others (see Introduction) to show that the characteristics of silver deposition on UV-illuminated TiO_2 allow one to envisage a practical use of this method. However, more research work is still necessary using, in particular, solutions that contain ions or complexes capable of competing with Ag^+ ions for adsorption on TiO_2. In some cases, prior pretreatments can be required to eliminate these elements, as has been shown for the recovery of gold in solutions containing cyanide ions (*12*). In addition, preliminary results have shown that silver can also be deposited on other powdered semiconductors, such as CdS, Fe_2O_3, and WO_3 using wavelengths in the visible spectral region.

ACKNOWLEDGMENTS

This work was supported by a special CNRS contract (A.T.P. PIRSEM No. 1036). We thank Mrs. Chambosse, Mr. H. Urbain, and Mrs. C. Leclercq of the Institut de Recherches sur la Catalyse–CNRS for some metal analyses and TEM/STEM examinations.

REFERENCES

1. Clark, W. C., and Vondjidis, A. G., *J. Catal.* **4,** 691 (1965).
2. Möllers, F., Tolle, H. J., and Memming, R., *J. Electrochem. Soc.* **121,** 1160 (1974).
3. Kelly, J. J., and Vondeling, J. K., *J. Electrochem. Soc.* **122,** 1103 (1975).
4. Krauetler, B., and Bard, A. J., *J. Amer. Chem. Soc.* **100,** 4317 (1978).
5. Sungbom, C., Kawai, M., and Tanaka, K., *Bull. Chem. Soc. Japan* **57,** 871 (1984).
6. Dunn, W. W., and Bard, A. J., *Nouv. J. Chim.* **5,** 651 (1981).
7. Stadler, K. H., and Boehm, H. P., "Proceedings, International Congress on Catalysis, 8th, Berlin, 1984," Vol. IV, p. 803. Dechema, Frankfurt-am-Main, 1984.
8. Sato, S., *J. Catal.* **92,** 11 (1985).
9. Nakamatsu, H., Kawai, T., Koreeda, A., and Kawai, S., *J. Chem. Soc. Faraday Trans. 1* **82,** 527 (1985).
10. Herrmann, J.-M., Disdier, J., Pichat, P., and Leclercq, C., *in* "Preparation of Catalysts IV" (B. Delmon, P. Grange, P. A. Jacobs, and G. Poncelet, Eds.), p. 285. Elsevier, Amsterdam, 1987.
11. Borgarello, E., Harris, R., and Serpone, N., *Nouv. J. Chim.* **9,** 743 (1985).
12. Serpone, N., Borgarello, E., Barbeni, M., Pelizzetti, E. Pichat, P., Herrmann, J.-M., and Fox, M. A., *J. Photochem.* **36,** 373 (1987).
13. Borgarello, E., Serpone, N., Emo, G., Harris, R., Pelizzetti, E., and Minero, C., *Inorg. Chem.* **25,** 4499 (1986).
14. Herrmann, J.-M., Disdier, J., and Pichat, P., *J. Phys. Chem.* **90,** 6028 (1986).
15. Korsunovskii, G. A., *Russ. J. Phys. Chem.* **39,** 1139 (1965).
16. Fleischauer, P. D., Alan Kan, H. K., and Shepherd, J. R., *J. Amer. Chem. Soc.* **94,** 283 (1972).
17. Hada, H., Tanemura, H., and Yonezawa, Y., *Bull. Chem. Soc. Japan* **51,** 3154 (1978).
18. Hada, H., Yonezawa, Y., and Saikawa, M., *Bull. Chem. Soc. Japan* **55,** 2010 (1982).
19. Hada, H., Yonezawa, Y., Ishino, M., and Tanemura, H., *J. Chem. Soc. Faraday Trans. 1* **78,** 2677 (1982).
20. Nishimoto, S., Ohtani, B., Kajiwara, H., and Kagiya, T., *J. Chem. Soc. Faraday Trans. 1* **79,** 2685 (1983).
21. Ohtani, B., Okugawa, Y., Nishimoto, S., and Kagiya, T., *J. Phys. Chem.* **91,** 3550 (1987).
22. Flaig-Baumann, R., Herrmann, M., and Böhm, H. P., *Z. Anorg. Allgem. Chem.* **372,** 296 (1970).
23. Van Damme, H., and Hall, W. K., *J. Amer. Chem. Soc.* **101,** 4373 (1979).
24. Herrmann, J.-M., "Proceedings, 9th Ibero-American Symposium on Catalysis, Jorge Fernandes, Lisbon," Vol. 1, p. 668, 1984.
25. Yoneyama, H., Nishimura, N., and Tamura, H., *J. Phys. Chem.* **85,** 268 (1981).
26. White, J. R., and O'Sullivan, E. J. M. *J. Electrochem. Soc.* **134,** 1133 (1987).
27. Egerton, T. A., and King, C. J., *J. Oil Col. Chem. Assoc.* **62,** 386 (1979).
28. Childs, L. P., and Ollis, D. F., *J. Catal.* **66,** 383 (1980).
29. Pichat, P., *in* "Photoelectrochemistry, Photocatalysis and Photoreactors" (M. Schiavello, Ed.), pp. 425–455. Reidel, Dordrecht, 1985.
30. Disdier, J., Herrmann, J.-M., and Pichat, P., *J. Chem. Soc. Faraday Trans. 1* **79,** 651 (1981).
31. Jacobs, J. W. M., *J. Phys. Chem.* **90,** 6507 (1986).